American Journal of Physical Chemistry
2021; 10(4): 111-118
http://www.sciencepublishinggroup.com/j/ajpc
doi: 10.11648/j.ajpc.20211004.18
ISSN: 2327-2430 (Print); ISSN: 2327-2449 (Online)

Implementation and Realization of a Kossel Diffraction Pattern Simulation Application

Fannou Jean-Louis Comlan[1, 2], Semassou Guy Clarence[1], Moussa Djibril Aliou[3], Gerbaud Patrice[4], Hougan Aristide[1]

[1]Laboratory of Applied Energy and Mechanics (LEMA), Polytechnic School of Abomey-Calavi, University of Abomey-Calavi, Cotonou, Benin

[2]National Higher School of Energy and Processes Engineering (ENSGEP), National University of Science, Technology, Engineering and Mathematics (UNSTIM), Abomey, Benin

[3]National Higher School of Mathematical Engineering and Modeling (ENSGMM)/ National University of Science, Technology, Engineering and Mathematics (UNSTIM), Abomey, Benin

[4]Laboratory of Thermodynamics, Electrical Properties, Stresses and Structures at Nanoscale (TECSEN), Université d'Aix-Marseille III, Marseille, France

Email address:
jlfannou@gmail.com (F. Jean-Louis C.)

To cite this article:
Fannou Jean-Louis Comlan, Semassou Guy Clarence, Moussa Djibril Aliou, Gerbaud Patrice, Hougan Aristide. Implementation and Realization of a Kossel Diffraction Pattern Simulation Application. *American Journal of Physical Chemistry*. Vol. 10, No. 4, 2021, pp. 111-118. doi: 10.11648/j.ajpc.20211004.18

Received: October 16, 2021; **Accepted**: November 8, 2021; **Published**: November 29, 2021

Abstract: To better understand some of the local metallurgical mechanisms, it is necessary to have information about the scale of the stress gradient in the vicinity of a grain boundary or around a precipitate. This measurement is accessible by Kossel microdiffraction. Diffraction consists of the emission of Kossel cones, which are then intercepted by a screen. This leads to an image that can be used to trace the deformation field. The simulation technique is best suited to this purpose. The present work falls within this framework and aims on the one hand to geometrically model the phenomenon and on the other hand to develop an application in Java language for digital simulations of the Kossel cliché. The methodology adopted is to take into account all the parameters on which the phenomenon depends to establish the geometric model which has been programmed in the JAVA language with a view to making a simulation application comprising 14 interacting classes. The result obtained after an example of simulation is rather satisfactory and promising. However, a comparison will have to be made for the complete validation of the model. This will be the subject of another publication later.

Keywords: Kossel Micro Diffraction, Cone, Observation Screen, Deformation Field, Image

1. Introduction

The enhancement of materials used in microelectronics, for example the crystals used in telephone chips, is of great importance today. It requires the evaluation of the physico-chemical behaviour of these materials, in real time, under stress. To this end, several exploratory methods have been developed. One of these methods is Kossel diffraction, which consists of sending an X-ray onto a crystal and using the Liquid Crystal Display (LCD) camera to recover the Kossel image resulting from the intersection of the diffraction cones with the observation plan. The objective is to go back to the deformation field by analyzing the Kossel image. The difficulty of exploiting this image has given rise to other approaches to solving the problem, including "image simulation", which seems to be the most obvious. Indeed, it will allow us to proceed by comparison or by recalibration. Several researchers have developed tools to help with the indexing of Kossel images. The first works consisted in simulating stereographic projection images. These include Lonsdale in 1947 [1], Hanneman et al. in 1962 [2] who prepared standard projections for crystallography and current radiation after calculation of Bragg angles. This led to the possibility of computer simulation of the images by Frazer [3]

and Morris [4] in 1966. Tixier and Waché [5] then indexed the lines of an experimental Kossel image for an iron crystal by comparison with a calculated projection. This technique is advantageous in that it is not necessary to know the center of the projection. Another example is the KOPSKO program developed by Langer et al [6]. The mesh parameters and material orientation must be entered by the user and a Kossel image is simulated based on classical diffraction relations and reference frame changes. Therefore, Weber has developed a program called KOQUA [7] that allows the simulation of Kossel images of all crystal structures. By comparing the experimental image with the simulated one, he can determine the lattice parameters to the nearest 0.005 Å by gradually varying the values within the program until an optimal match between the two images is obtained. In 2006, Pesci et al [8] implemented a software program allowing the determination of the orientation of Kossel plates and the estimation of deformations by comparing an experimental plate with its simulated equivalent. Finally, more recently, Denis BOUSCAUD [9] presented a methodology to perform the analysis of experimental images by using and improving a software that uses a semi-automatic procedure for the absolute determination of six components of tensor deformations. The operator has to manually position points on the image to determine the reflection position. By comparing two images, it is possible to deduce the relative state of deformation from an automatic correlation of the line profiles. J.-M. André et al [10] shown that by combining the reciprocity theorem, the Fermi golden rule and the concept of density of photonic modes, it is possible to predict the behaviour of the Kossel diffraction in such a system. Similarly Meiyi Wu, Karine Le Guen, Jean-Michel André, Philippe Jonnard, Ian Vickridge, et al [11], has shown that by combining Kossel diffraction with particle induced X-ray emission, we have developed a new methodology to analyze nano-scale thin films.

These different works, although they allowed the simulation of the Kossel image, did not take into account all the parameters and are a little outdated, given the permanent evolution of the technology. The work presented here is part of the same dynamic and aims to implement a graphic interface and the processing tools necessary for a slightly more optimal simulation of a Kossel image.

2. Materials and Methods

2.1. Materials

The Kossel microdiffraction technique is a radio crystallographic method in which X-rays, emitted when an incident beam of electrons interacts with the material (crystal), are diffracted by the crystal lattice and emerge from the material forming a cone (see figure 1a). The intersection of the cones with a film plan gives diffraction lines. The set of diffraction lines forms the Kossel pattern (Figure 1b). The determination of the state of stress is based on the measurement of the lattice distances of the diffraction plans. The accuracy of this measurement depends essentially on the accuracy of the reading of the position of the lines on the image.

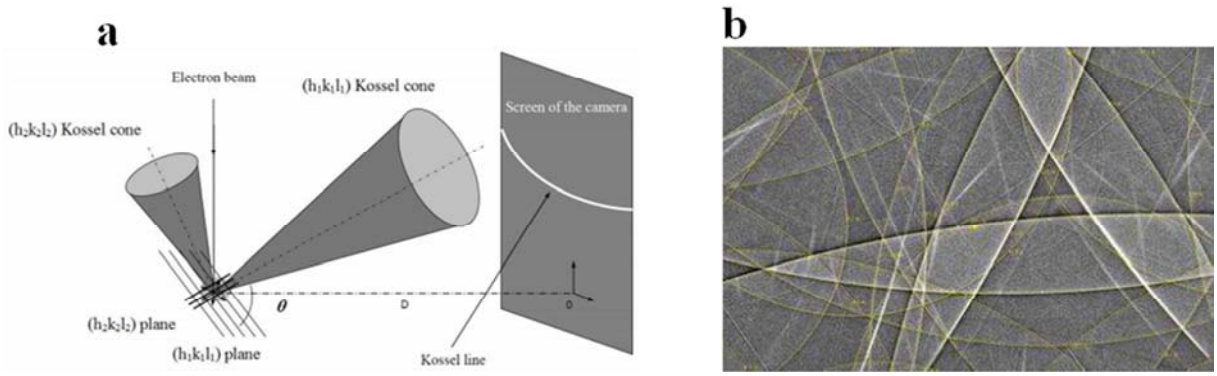

Figure 1. *Kossel microdiffraction technique. (a) Principle of emission from Kossel diffraction cones [9]. (b) Kossel analysis of a grain on a copper deposit [12, 13].*

The experimental set-up for the acquisition of Kossel diffraction images, installed in the TECSEN (Thermodynamics, Electrical Properties, Stresses and Structures at Nanoscale) laboratory, is shown in Figure 2. It is essentially made up of an electron microscope and microanalysis (all scales), a lifetime and wavelength measurement and mapping system, a Focused Ion Beam (silicon micromachining), a system for measuring mechanical stresses in thin films, an all-temperature micro-calorimetry system, a heat treatment furnace and an X-ray diffraction system.

Figure 2. *TECSEN test and measurement device.*

2.2. Methods

2.2.1. Data

In order to model and simulate the Kossel diffraction pattern, the model input parameters from the experimental pattern were used:

1) Crystal orientation in the sample frame characterized by the crystal orientation directions: $u, v, w, p, q, r, H, K, L$

$$\begin{bmatrix} u & p & H \\ v & q & K \\ w & r & L \end{bmatrix} \quad (1)$$

2) Tensor of elastic constants C_0 in the base of the (100)(010)(001) crystal (experimental data)

$$C_0 = \begin{bmatrix} C_{11} & C_{12} & C_{12} & 0 & 0 & 0 \\ C_{12} & C_{11} & C_{12} & 0 & 0 & 0 \\ C_{12} & C_{12} & C_{11} & 0 & 0 & 0 \\ 0 & 0 & 0 & C_{44} & 0 & 0 \\ 0 & 0 & 0 & 0 & C_{44} & 0 \\ 0 & 0 & 0 & 0 & 0 & C_{44} \end{bmatrix} \Longrightarrow$$

$$S_0 = {C_0}^{-1} = \begin{bmatrix} S_{11} & S_{12} & S_{12} & 0 & 0 & 0 \\ S_{12} & S_{11} & S_{12} & 0 & 0 & 0 \\ S_{12} & S_{12} & S_{11} & 0 & 0 & 0 \\ 0 & 0 & 0 & S_{44} & 0 & 0 \\ 0 & 0 & 0 & 0 & S_{44} & 0 \\ 0 & 0 & 0 & 0 & 0 & S_{44} \end{bmatrix} \quad (2)$$

3) Stress tensor in measurement basis $(uvw)(pqr)(HKL)$

$$\sigma_m = \begin{bmatrix} \sigma_{11} & \sigma_{12} & \sigma_{13} \\ \sigma_{12} & \sigma_{22} & \sigma_{23} \\ \sigma_{13} & \sigma_{23} & \sigma_{33} \end{bmatrix} \Longrightarrow \overline{\sigma_m} = \begin{bmatrix} \overline{\sigma_{11}} \\ \overline{\sigma_{22}} \\ \overline{\sigma_{33}} \\ \overline{\sigma_{23}} \\ \overline{\sigma_{13}} \\ \overline{\sigma_{12}} \end{bmatrix} \quad (3)$$

2.2.2. Calculations

From the above input data, we calculate:

1) the base changing matrix with normalized vectors:

$$\begin{bmatrix} \frac{u}{\sqrt{u^2+v^2+w^2}} & \frac{p}{\sqrt{p^2+q^2+r^2}} & \frac{H}{\sqrt{H^2+K^2+L^2}} \\ \frac{v}{\sqrt{u^2+v^2+w^2}} & \frac{q}{\sqrt{p^2+q^2+r^2}} & \frac{K}{\sqrt{H^2+K^2+L^2}} \\ \frac{w}{\sqrt{u^2+v^2+w^2}} & \frac{r}{\sqrt{p^2+q^2+r^2}} & \frac{L}{\sqrt{H^2+K^2+L^2}} \end{bmatrix} \quad (4)$$

2) the transpose base changing matrix:

$$\begin{bmatrix} \frac{u}{\sqrt{u^2+v^2+w^2}} & \frac{v}{\sqrt{u^2+v^2+w^2}} & \frac{w}{\sqrt{u^2+v^2+w^2}} \\ \frac{p}{\sqrt{p^2+q^2+r^2}} & \frac{q}{\sqrt{p^2+q^2+r^2}} & \frac{r}{\sqrt{p^2+q^2+r^2}} \\ \frac{H}{\sqrt{H^2+K^2+L^2}} & \frac{K}{\sqrt{H^2+K^2+L^2}} & \frac{L}{\sqrt{H^2+K^2+L^2}} \end{bmatrix} = \begin{bmatrix} m_{11} & m_{12} & m_{13} \\ m_{21} & m_{22} & m_{23} \\ m_{31} & m_{32} & m_{33} \end{bmatrix} \quad (5)$$

3) Angot's basis changing matrix [14]:

$$M = \begin{bmatrix} {m_{11}}^2 & {m_{12}}^2 & {m_{13}}^2 & 2m_{12}m_{13} & 2m_{11}m_{13} & 2m_{11}m_{12} \\ {m_{21}}^2 & {m_{22}}^2 & {m_{23}}^2 & 2m_{22}m_{23} & 2m_{21}m_{23} & 2m_{21}m_{22} \\ {m_{31}}^2 & {m_{32}}^2 & {m_{33}}^2 & 2m_{32}m_{33} & 2m_{31}m_{33} & 2m_{31}m_{32} \\ m_{21}m_{31} & m_{22}m_{32} & m_{23}m_{33} & m_{22}m_{33}+m_{32}m_{23} & m_{21}m_{33}+m_{31}m_{23} & m_{21}m_{32}+m_{31}m_{22} \\ m_{11}m_{31} & m_{12}m_{32} & m_{13}m_{33} & m_{12}m_{33}+m_{32}m_{13} & m_{11}m_{33}+m_{31}m_{13} & m_{11}m_{32}+m_{31}m_{12} \\ m_{11}m_{21} & m_{12}m_{22} & m_{13}m_{23} & m_{12}m_{23}+m_{22}m_{13} & m_{11}m_{23}+m_{21}m_{13} & m_{11}m_{22}+m_{21}m_{12} \end{bmatrix} \quad (6)$$

4) Stress tensor in the crystal base $(100)(010)(001)$:

$$\overline{\sigma_0} = (M)^{-1}(\overline{\sigma_m}) \quad (7)$$

5) Deformation tensor in the base of the crystal $(100)(010)(001)$:

$$\overline{\varepsilon_0} = S_0\overline{\sigma_0} = \begin{bmatrix} {\varepsilon^0}_{11} \\ {\varepsilon^0}_{22} \\ {\varepsilon^0}_{33} \\ 2{\varepsilon^0}_{23} \\ 2{\varepsilon^0}_{13} \\ 2{\varepsilon^0}_{12} \end{bmatrix} \Longrightarrow \varepsilon_0 = \begin{bmatrix} {\varepsilon^0}_{11} & {\varepsilon^0}_{12} & {\varepsilon^0}_{13} \\ {\varepsilon^0}_{12} & {\varepsilon^0}_{22} & {\varepsilon^0}_{23} \\ {\varepsilon^0}_{13} & {\varepsilon^0}_{23} & {\varepsilon^0}_{33} \end{bmatrix} \quad (8)$$

6) Inverse metric tensor of the deformed crystal

$$GI = \frac{1}{a_0^2}\,(\delta - 2\varepsilon_0)\; avec\; \delta = \begin{bmatrix} 1 & 0 & 0 \\ 0 & 1 & 0 \\ 0 & 0 & 1 \end{bmatrix}$$

$$GI = \frac{1}{a_0^2}\begin{bmatrix} 1-2{\varepsilon^0}_{11} & 2{\varepsilon^0}_{12} & 2{\varepsilon^0}_{13} \\ 2{\varepsilon^0}_{12} & 1-2{\varepsilon^0}_{22} & 2{\varepsilon^0}_{23} \\ 2{\varepsilon^0}_{13} & 2{\varepsilon^0}_{23} & 1-2{\varepsilon^0}_{33} \end{bmatrix} = \begin{bmatrix} GI_{11} & GI_{12} & GI_{13} \\ GI_{12} & GI_{22} & GI_{23} \\ GI_{13} & GI_{23} & GI_{23} \end{bmatrix} \quad (9)$$

7) The interreticular distance is given by:

$$\frac{1}{d_{hkl}^2} = \begin{bmatrix} h^2 & k^2 & l^2 & 2hk & 2kl & 2hl \end{bmatrix}\begin{bmatrix} GI_{11} \\ GI_{22} \\ GI_{33} \\ GI_{12} \\ GI_{23} \\ GI_{13} \end{bmatrix} \quad (10)$$

8) The angle at the top of the cone (hkl) is given by:

$$\alpha = \frac{\pi}{2} - \arcsin\left(\frac{\lambda}{2d_{hkl}}\right) \quad (11)$$

2.2.3. Geometric Modelling

The mathematical model of the experimental setup is as follows:

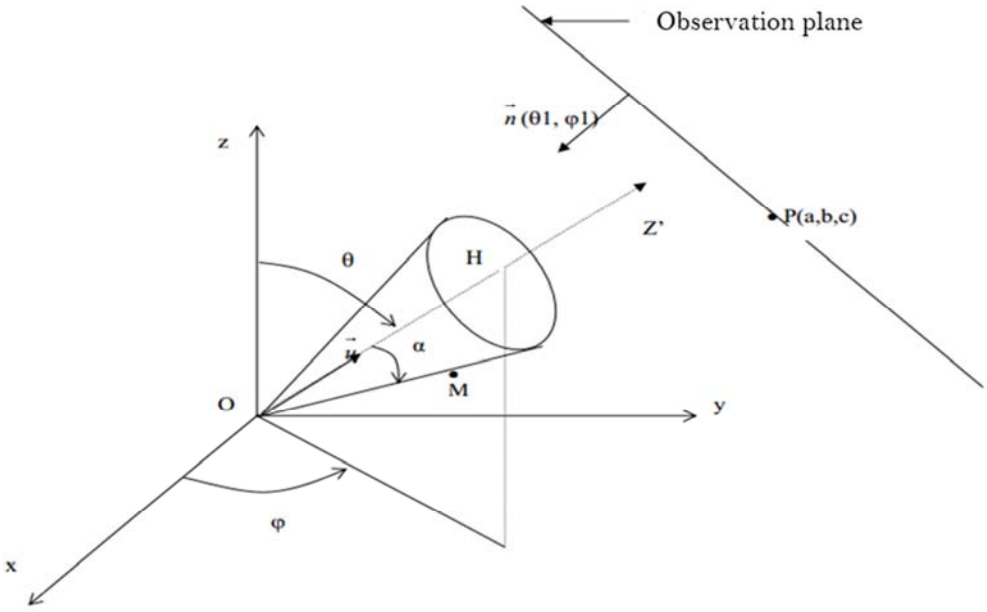

Figure 3. *Model of the experimental set-up (crystal related).*

In order to simplify the equations that would be implied by the geometrical model of the experimental set-up, geometrical transformations are necessary. The first step was to write the equations of the cone and the plan in the reference frame related to the crystal.

Always, for any point M(x,y,z) of a cone of revolution of half angle at vertex α:

$$\overrightarrow{OM}.\vec{u} = \alpha \tag{12}$$

$$\cos(\alpha) = \frac{\overrightarrow{OM}.\vec{u}}{\|\overrightarrow{OM}\|.\|\vec{u}\|} \tag{13}$$

By squaring the relation (13) and replacing the different terms with their expressions:

$$\overrightarrow{OM} = x\vec{\imath} + y\vec{\jmath} + z\vec{k}$$

$$\vec{u} = \begin{cases} sin\theta.\cos\varphi \\ sin\theta.sin\varphi \\ cos\theta \end{cases}$$

The equation of the cone becomes:

$$cos^2(\alpha)(x^2 + y^2 + z^2) = (xsin\theta.\cos\varphi + ysin\theta.sin\varphi + zcos\theta)^2 \tag{14}$$

Furthermore, as the normal vector $\vec{n}\,(\theta_1, \varphi_1)$ and a point $P(a, b, c)$ of the plan which are the parameters given by the user are known, the plan equation is:

$$(x-a)sin\theta_1.cos\varphi_1 + (y-b)sin\theta_1.sin\varphi_1 + (z-c)cos\theta_1 = 0 \tag{15}$$

As these equations are a bit complex, we thought of performing a double rotation in order to simplify them. For the cone, it will be done in such a way as to make the axis z coincide with the axis of the cone. Successively, a rotation of angle $-\varphi$ of the axis x around the axis z translating the passage from the reference frame (x, y, z) to the reference frame (x', y', z') and a rotation of angle $-\theta$ of the axis z around the axis y' translating the passage from the reference frame (x', y', z) to the reference frame (X', Y', Z') allowed to obtain a more simplified equation for the cone.

Let M_1 and M_2 be the matrices of these different rotations. We have:

$$M_1 = \begin{pmatrix} cos\varphi & sin\varphi & 0 \\ -sin\varphi & cos\varphi & 0 \\ 0 & 0 & 1 \end{pmatrix} \tag{16}$$

$$M_2 = \begin{pmatrix} cos\theta & 0 & -sin\theta \\ 0 & 1 & 0 \\ sin\theta & 0 & cos\theta \end{pmatrix} \tag{17}$$

Assuming $R = M_2.M_1$, the formulas for the change of reference frame are written:

$$\begin{pmatrix} x \\ y \\ z \end{pmatrix} = R^{-1}\begin{pmatrix} X' \\ Y' \\ Z' \end{pmatrix} \tag{18}$$

The development of (18) gives:

$$\begin{cases} x = X'cos\theta.cos\varphi - Y'sin\varphi + Z'cos\varphi.sin\theta \\ y = X'cos\theta.sin\varphi - Y'cos\varphi + Z'sin\varphi.sin\theta \\ z = -X'sin\theta + Z'cos\varphi.sin\theta \end{cases} \quad (19)$$

Substituting equations (19) into equation (14) and knowing that $1 + tan^2\alpha = \frac{1}{cos^2\alpha}$, the cone equation is simply written:

$$X'^2 + Y'^2 = Z'^2 tan^2\alpha \quad (20)$$

In the same way, we obtain the new equation of the plan:

$$a'X' + b'Y' + c'Z' = d' \quad (21)$$

with:

$$\begin{cases} a' = sin\theta_1.cos\ \varphi_1.cos\theta.cos\varphi + sin\theta_1.sin\ \varphi_1.cos\theta.sin\varphi - cos\theta_1 sin\theta \\ b' = -sin\theta_1.cos\ \varphi_1.sin\varphi + sin\theta_1.sin\ \varphi_1.cos\varphi \\ c' = sin\theta_1.cos\ \varphi_1.sin\theta.cos\varphi + sin\theta_1.sin\ \varphi_1.sin\theta.sin\varphi + cos\theta_1 cos\theta \\ d' = sin\theta_1.cos\ \varphi_1.a + sin\theta_1.sin\ \varphi_1.b - cos\theta_1.c \end{cases} \quad (22)$$

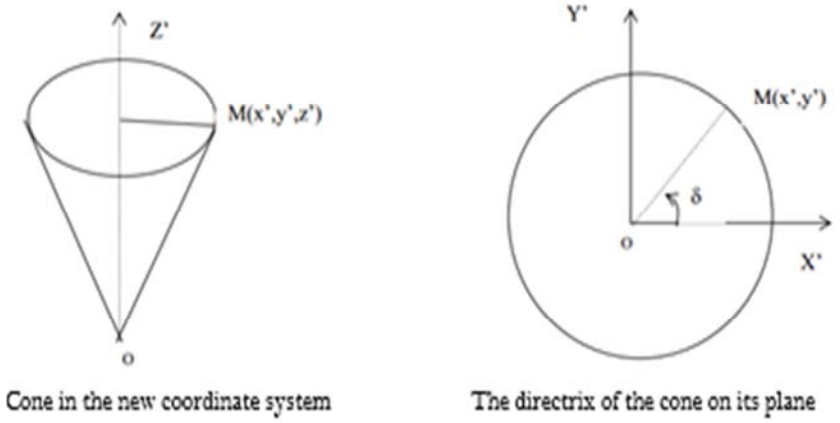

Figure 4. *Cone Observation.*

For the system formed by equations (20) and (21) cannot be solved analytically, it was felt that the conic could be obtained from the points of intersection of each of the cone generatrices with the plan. The graphical representation of these points provides the shape of the conic. It should be noted that in general the section of a cone with a plane gives conics.

The radius of the directrix of the cone has the expression:

$$R = z'tan\alpha \quad (23)$$

The coordinates of a point M on the cone are then:

$$\begin{cases} x' = z'tan\alpha.cos\delta \\ y' = z'tan\alpha.sin\delta \\ z' = z' \end{cases} \quad (24)$$

The position vector of point M is written:

$$\overrightarrow{OM} = z'\vec{v} \quad (25)$$

$$\text{with } \vec{v} \begin{cases} x' = tan\alpha.cos\delta \\ y' = tan\alpha.sin\delta \\ z' = 1 \end{cases} \quad (26)$$

Putting $z' = t$, t a parameter, the parametric equations of the generators are:

$$\begin{cases} x' = t.tan\alpha.cos\delta \\ y' = t.tan\alpha.sin\delta \\ z' = t \end{cases} \quad (27)$$

Carrying equation (27) into equation (21), we derive the set of values of t, which determine, as a function of the values of δ, the number of generatrices and consequently the number of points of intersection of the cone with the plane:

$$t_\delta = \frac{d'}{a'tan\alpha.cos\delta + b'tan\alpha.sin\delta + c'} \quad (28)$$

By injecting (28) into (27), we obtain the general equations of the coordinates of the intersection points.

$$\begin{cases} x' = t_\delta.tan\alpha.cos\delta \\ y' = t_\delta.tan\alpha.sin\delta \\ z' = t_\delta \end{cases} \quad (29)$$

The observation screen is the plan. Knowing a normal vector $\overrightarrow{n_1}$to the plan, we need to choose two other vectors $\overrightarrow{n_2}, \overrightarrow{n_3}$ such that the coordinate system is direct orthonormal. These two vectors are generated by the application. It is then necessary to determine the new coordinates of the points of intersection in this new reference frame. By setting M_3, the matrix of passage from the reference frame $(\overrightarrow{n_1}, \overrightarrow{n_2}, \overrightarrow{n_3})$ to the reference frame $(\overrightarrow{X'}, \overrightarrow{Y'}, \overrightarrow{Z'})$, we have:

$$\begin{pmatrix} \overrightarrow{X'} \\ \overrightarrow{Y'} \\ \overrightarrow{Z'} \end{pmatrix} = {M_3}^{-1} \begin{pmatrix} \overrightarrow{n_1} \\ \overrightarrow{n_2} \\ \overrightarrow{n_3} \end{pmatrix} \quad (30)$$

By carrying (30) in (28), we obtain the new coordinates of the points of intersection of the plan with the cone.

3. Results and Analysis

An application was implemented to carry out the

simulations [15, 16]. It was entirely developed in Java, which is a language dedicated to object-oriented programming. The application program consists of 14 classes. It follows the following structure:

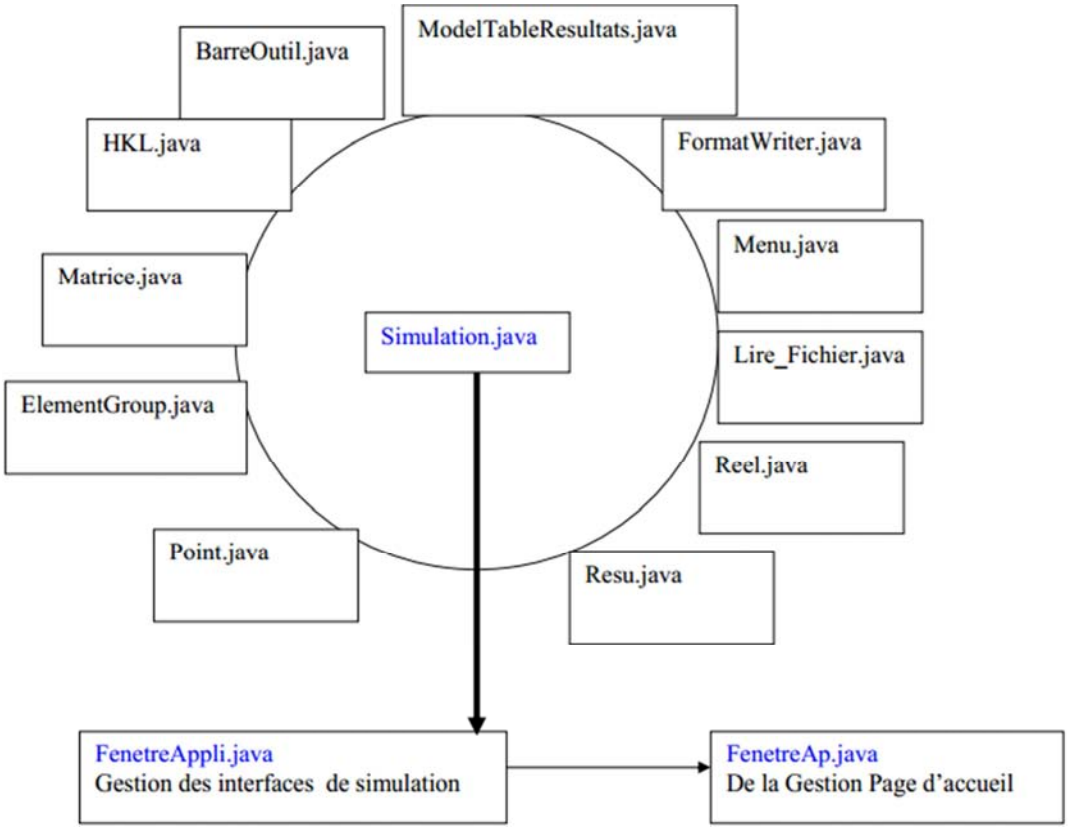

Figure 5. *Structure of the application.*

Figure 6a is a brief presentation of the home window of the software.

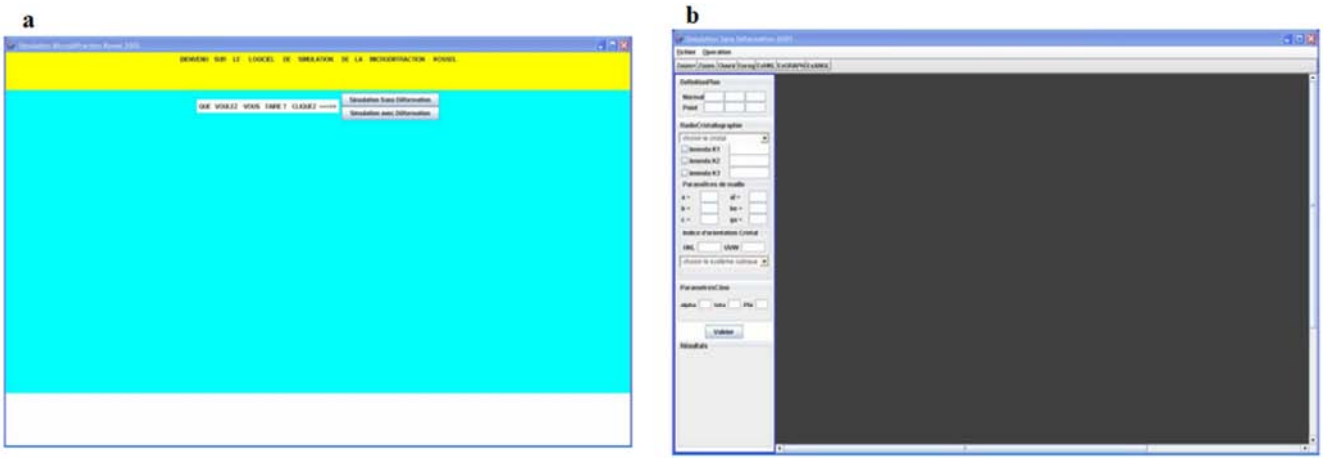

Figure 6. *Simulation interface of the Kossel diffraction pattern (a). Deformation-free simulation interface (b).*

It has two buttons to select the type of simulation: with or without deformation.

Figure 6b is the simulation interface without deformation.

For data entry and validation, the deformation-free simulation interface has two main groups of input fields:

1. "DefinitionPlan", which allows the observation plan to be modelled;
2. "RadioCristallography" which models the crystal mesh, its orientation and allows the choice of the cubic system.

The simulation interface with deformation (Figure 7a) is almost the same as before except that it has another group of input fields "Tensor Components (MPa)" which allows stresses to be taken into account.

In addition to the usual menus and submenus, the application has an "Operation" menu for performing simulation operations.

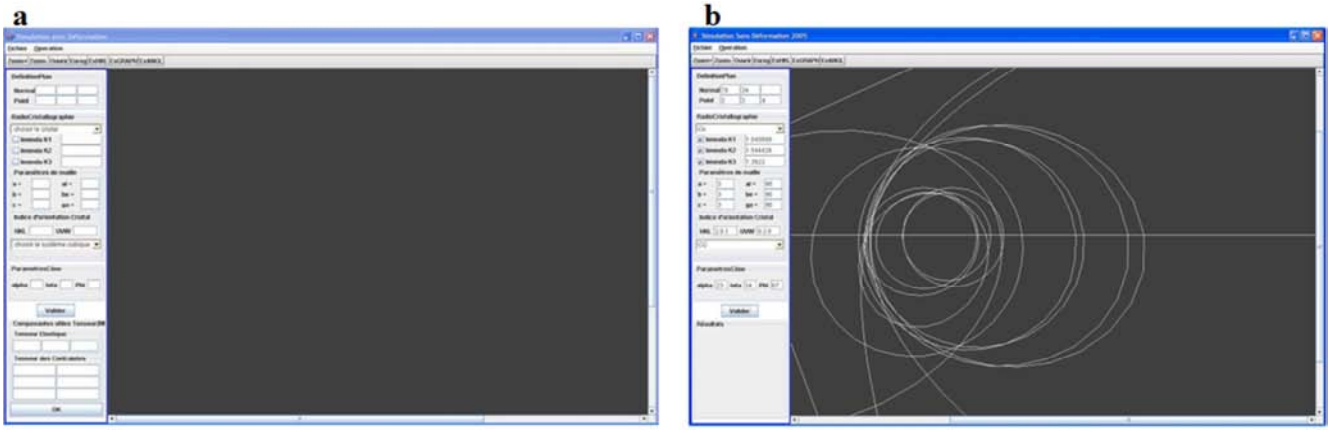

Figure 7. *Simulation. Example of simulation with deformation (a). Example of simulation without deformation (b).*

The figure 7b shows an example of simulation of a Kossel diffraction pattern which, compared to the one of figure 1b prove that the models presented here seems to answer to be satisfactory.

4. Conclusion

This study's goals were to implement and realize a Kossel diffraction pattern simulation application. Simulation is a very important step in the exploitation of Kossel images. In this respect, the work presented here has led to the implementation of an application. It already makes it possible to simulate a Kossel image with or without deformation. Nevertheless, it remains a first attempt and still has many shortcomings. It is thus called upon to evolve and to take into account the other crystal systems, the improvement of the graphic interface, the optimisation of codes, the improvement of the display function of the Kossel images, the indexing of the conics of the Kossel image etc. It should be noted, however, that this is a significant step forward in the optimal use of the Kossel image.

Nomenclature

$\vec{u}$	Unit vector on the cone axis
$\vec{v}$	Director vector of a generatrix for fixed
$\vec{n}$	Normal vector
t	A parameter
α	Half angle at the apex of the cone
P	A point in the observation plan

References

[1] Lonsdale, K. (1947). The divergent X-ray photography of crystals. Philosophical Transactions of the Royal Society A. Vol. 240, 219-258.

[2] Hanneman, R. E., Ogilvie, R. E., Modrzejewski, A. (1962). Kossel line studies of irradiated nickel crystals. Journal of Applied Physics. Vol. 33.

[3] Frazer, J., Arrhenius, G. (1966). Divergent-beam diffraction geometry for interpretation of Kossel diffraction patterns in space group assignment lattice parameters and structure factor evaluation. X-ray Optics and Microanalysis. Edition Hermann.

[4] Morris, W. G. (1968). Crystal orientation and lattice parameters from Kossel lines. Journal of Applied Physics. Vol. 39.

[5] Tixier, R., Waché, C. (1970). Kossel patterns. Journal of Applied Crystallography. Vol. 3, 466-485.

[6] Langer, E., Kurt, R., Däbritz, S. (1999). KOPSKO: a computer program for generation of Kossel and pseudo-Kossel diffraction patterns. Crystal Research and Technology. Vol. 34, 801-816.

[7] Weber, S., Schetelich, Ch., Geist, V. (1994). Computer-aided evaluation of Kossel patterns obtained from quasicrystals. Crystal Research and Technology. Vol. 29, 727-735.

[8] Pesci, R., Inal, K., Berveiller, S., Patoor, E., Lecomte, J. S., Eberhardt, A. (2006). Inter and intra granular stress determination with Kossel microdiffraction in a scanning electron microscope. Materials Science Forum. Vol. 524-525, 109-114.

[9] Denis BOUSCAUD, Thèse: Développement de la microdiffraction Kossel pour l'analyse des déformations et contraintes à l'échelle du micromètre - Applications à des matériaux cristallins (Thesis: Development of Kossel microdiffraction for the analysis of deformations and stresses at the micrometer scale - Applications to crystalline materials), 2012.

[10] J._M André, P. Jonnard, K. Le Guen, F. Bridou, Kossel diffraction and photonic modes in one-dimensional photonic cristal, PACS numbers 78.67. Pt, 78-70. En, 42.70 Qs, 61-05 C, 2015.

[11] Meiyi Wu, Karine Le Guen, Jean-Michel André, Philippe Jonnard, Ian Vickridge, et al.. Kossel diffraction observed with X-ray color camera during PIXE of nano-scale periodic multilayer. Nuclear Instruments and Methods in Physics Research Section B: Beam Interactions with Materials and Atoms, Elsevier, 2019, 450, pp. 252-256.

[12] D. Bouscaud, S. Berveiller, R. Pesci, C. Rivero, K. Inal, C. Maurice, R. Fortunier, K. Dzieciol, R. Vayrette, Hétérogénéités de contraintes intragranulaires: Détermination par approche couplée EBSD-Kossel (Heterogeneities of intragranular constraints: Determination by coupled EBSD-Kossel approach), 20ème Congrès Français de Mécanique, Besançon, 29 août au 2 septembre 2011.

[13] Faigel, G, G. Bortel, M. Tegze, Experimental phase determination of the structure factor from Kossel, line profile. *Sci. Rep.* 6, 22904; doi: 10.1038/srep22904, 2016.

[14] André ANGOT, Compléments de Mathématiques à l'usage des ingénieurs de l'électrotechnique et des télécommunications (Mathematics Complements for the Use of Electrical and Telecommunications Engineers), Paris, 1957.

[15] Henri Garreta, Fascicule de cours: Langage Java (Course booklet: Java language), 2004.

[16] Ivor Horton, Beginning Java 2-JDK 1.3, Edition, Wrox Press, 2001.